

# Control-Coherent Koopman Modeling: A Physical Modeling Approach

H. Harry Asada\*, *Life Fellow*, and Jose A. Solano-Castellanos

**Abstract**—The modeling of nonlinear dynamics based on Koopman operator theory, which is originally applicable only to autonomous systems with no control, is extended to non-autonomous control system without approximation to input matrix  $B$ . Prevailing methods using a least square estimate of the  $B$  matrix may result in an erroneous input matrix, misinforming the controller about the structure of the input matrix in a lifted space. Here, a new method for constructing a Koopman model that comprises the exact input matrix  $B$  is presented. A set of state variables are introduced so that the control inputs are linearly involved in the dynamics of actuators. With these variables, a lifted linear model with the exact control matrix, called a Control-Coherent Koopman Model, is constructed by superposing control input terms, which are linear in local actuator dynamics, to the Koopman operator of the associated autonomous nonlinear system. The proposed method is applied to multi degree-of-freedom robotic arms and multi-cable manipulation systems. Model Predictive Control is applied to the former. It is demonstrated that the prevailing Dynamic Mode Decomposition with Control (DMDc) using an approximate control matrix  $B$  does not provide a satisfactory result, while the Control-Coherent Koopman Model performs well with the correct  $B$  matrix.

**Index Terms**—Koopman lifting linearization; Koopman operator for control systems; Model predictive control

## I. INTRODUCTION

KOOPMAN Operator theory has the potential to be a breakthrough in representation of complex nonlinear dynamics. A globally linear, unified representation facilitates control synthesis and analysis. Powerful linear systems theory and techniques can be applied to complex nonlinear systems. It has already had significant impacts upon various branches of control theory and applications, ranging from system identification [1], Model Predictive Control [2], and robust control [3] to soft robot modeling and control [4], vehicle control [5], and active robot learning [6].

Despite promising reports, a fundamental problem has not yet been solved. Is Koopman operator theory applicable to non-autonomous systems with control? The Koopman Operator theory is originally applicable only to autonomous systems having no exogenous input [7, 8]. Almost all control systems are non-autonomous with control, to which the Koopman theory does not apply in the strict sense. Criticisms of the Koopman Operator approach often pertain to this limitation.

The Koopman research community has been attempting to remove this limitation. An ad hoc method is to simply approximate the control input term to a linear term with constant coefficients,  $\dot{z} = Az + Bu$ , where  $z$  is lifted state and  $u$  is input. Matrices  $A$  and  $B$  are obtained from least square estimation. The method referred to as Dynamic Mode Decomposition with Control (DMDc) is in this category [9]. Assuming a constant matrix  $B$  is difficult to justify because the coefficients are state dependent in many nonlinear systems. Although state variables can be lifted for global linearization, control variables cannot, because the number of independent input variables is physically determined.

The second method is to treat control inputs as part of the independent state variables and apply the standard Koopman Operator to the augmented state variables,  $(x^T, u^T)^T$  [10]. This entails a prescribed differential equation governing the time evolution of control  $u$ . This method cannot be used for designing a controller from a model because the control is determined before the Koopman Model is obtained. This formulation results in a causality violation in most control design settings.

A more rigorous and more accurate method is to use a bilinear formulation. Due to the state-dependent nature of control input terms, it is difficult to approximate it to linear terms. Instead, these can be more accurately approximated to bilinear terms, where the control input terms are modeled as products of state variables and control variables [11]. This bilinear approximation provides a much more accurate approximation, but the resultant Koopman model is not linear but bilinear; it is more restrictive and complex, compared to the completely linear Koopman model.

Here, we present a method for constructing a Koopman operator for a class of control systems without approximation of the input matrix  $B$ . Integrity and coherency of the input matrix are crucial for proper control design. A control matrix that is determined merely by curve fitting to data may not have the right structure, which may misinform control design. The proposed method guarantees the coherent, correct structure by construction. No curve fitting to a linear or bilinear parametric model is used. The method is based on causality of physical system modeling applied to actuator power-train dynamics. The new method will fill the theoretical and technical gap between the Koopman operator theory and what is needed in control engineering. The method is applicable to a vast number of control systems. A few concrete examples will manifest the

usefulness of the method for controlling practical systems.

## II. BACKGROUND AND PROBLEM FORMULATION

Consider a discrete-time, nonlinear dynamical system given by

$$x_{t+1} = f(x_t, u_t) \quad (1)$$

where  $x_t \in X \subset \mathcal{R}^n$  is independent state,  $u_t \in U \subset \mathcal{R}^r$  is input, and  $f$  is a continuously differentiable function,  $f: (X, U) \mapsto X$  defined in compact sets  $X$  and  $U$ . The autonomous system associated to (1) is

$$x_{t+1} = F(x_t) \quad (2)$$

where  $u_t \equiv 0$  and the function  $F$  is a self-map,  $F: X \mapsto X$ .

Let  $\{g_i(x_t)\}_{i=1}^\infty$  be observables that span a Hilbert space  $\mathcal{H}$ . Assume that the observables compositional with the self-map  $F$  are involved in the Hilbert space.

$$g_i \circ F \in \mathcal{H}, \quad i = 1, 2, \dots \quad (3)$$

Then, the following Koopman operator  $A$  exists:

$$z_{t+1} = Az_t \quad (4)$$

where  $z_t = (g_1(x_t), g_2(x_t), \dots)^T$  is the infinite-dimensional state lifted with  $\{g_i\}_{i=1}^\infty$  [7, 12].

The Koopman operator can be obtained with various methods. The most prevailing is the extended dynamic mode decomposition (eDMD), which is based on least square estimate and singular value decomposition. A more rigorous method is to obtain the Koopman operator from inner products of the observables and their composition with the self-map, state transition function  $F$ . Post-multiply  $z_t^T$  to both sides of (4) and integrate them over the dynamic range of the independent state yields

$$Q = AR \quad (5)$$

where

$$Q = \langle z_{t+1}, z_t^T \rangle = \left\{ \int_X g_i[F(x)] \cdot g_j(x) dx \right\} \quad (6)$$

$$R = \langle z_t, z_t^T \rangle = \left\{ \int_X g_i(x) \cdot g_j(x) dx \right\} \quad (7)$$

The Koopman operator is the solution to the linear equation (5). This method directly encodes the state transition function  $F$  with a given set of observables  $\{g_i\}_{i=1}^\infty$ , called Koopman Direct Encoding [12].

Finding an effective set of observables is a challenge. Among others, the use of deep learning is a promising data-driven method for finding observables that can approximate the Koopman operator with a lower dimensional model [13-16].

Those methods established in the Koopman Operator theory are for autonomous systems with no control input. The objective of this paper is to develop a Koopman lifted linearization method for the non-autonomous system (1) in the

following form:

$$z_{t+1} = Az_t + Bu_t. \quad (8)$$

which is linear in control  $u_t$  with a constant input matrix  $B$ .

In the DMDc method, the  $A$  and  $B$  matrices are given by

$$(\hat{A}, \hat{B}) = \arg \min_{A, B} \sum |z_+(i) - (Az_-(i) + Bu_-(i))|^2 \quad (9)$$

where the  $A$  and  $B$  matrices are fitted to data  $\{(z_+(x(i)), z_-(x(i)), u_-(i)) | i = 1, \dots, N\}$  consisting of before ( $z_-$ ,  $u_-$ ) and after  $z_+$  each transition. In this formulation, the input matrix  $B$  is determined simply by minimizing the squared error. Note that the nonlinear dynamics with regard to the state  $x_t$  can be globally linearized by lifting the state. However, it does not apply to the input  $u$ . This may cause an incoherent input matrix  $B$ , although the curve fitting shows a good agreement. The method proposed can solve these problems.

## III. CONTROL-COHERENT KOOPMAN MODELING

Control systems are activated with actuators that drive some state variables directly in response to control input. We divide the state space into the one associated to a set of state variables  $p_t \in P \subset \mathcal{R}^m$  that is driven directly with input  $u_t$  and the rest of the state variables  $q_t \in \mathcal{R}^{n-m}$  that are not directly driven by  $u_t$  but indirectly through  $p_t$ .

$$x_t = \begin{bmatrix} p_t \\ q_t \end{bmatrix}. \quad (10)$$

**Definition 1** [Actuation Subsystem]

The dynamical system (1) is said to have an actuation subsystem if the state equation (1) can be divided into the following two:

$$p_{t+1} = f_p(x_t, u_t) \quad (11)$$

$$q_{t+1} = f_q(x_t) \quad (12)$$

where  $f_q: X \mapsto X_q \subset \mathcal{R}^{n-m}$  and  $f_p: (X, U) \mapsto P$  are continuously differentiable, and  $u_t$  is involved in each component  $f_{p,i}$ ,

$$\frac{\partial f_{p,i}}{\partial u_t} \neq 0, i = 1, \dots, m \quad (13)$$

In the following derivation, we are interested in an actuator subsystem that is nonlinear in state  $x_t$  but is linear in input  $u_t$ .

**Definition 2** [Linear Actuation]

If the actuation subsystem involved in the dynamical system (1) is in the following form,

$$p_{t+1} = h(x_t) + B_p u_t \quad (14)$$

the system is said to be linear in actuation.

**Remark 1**

As will be discussed further in the following examples, actuation subsystems are linear in control in most electro-

mechanical systems. A DC motor and a brushless DC motor, for example, have equations of motion given by:

$$I\ddot{\phi} = \tau_m - \tau_{load} \quad (15)$$

where  $\phi$  is rotor displacement,  $I$  is the rotor inertia,  $\tau_m$  is the torque generated by the actuator, and  $\tau_{load}$  is the load torque as the actuator is engaged with a load. Treating  $\tau_m$  as input yields an actuator subsystem that is linear in actuation.

**Remark 2**

The actuation subsystem must have independent state variables  $p$ . This requirement can be met in several ways. For example, if the power train connecting an actuator to its load has a compliance, the local actuator subsystem and the main system driven via the power train can possess independent state variables,  $p$  and  $q$ . These independent state variables are dynamically coupled through, for example, the power train having a coupling impedance.

A Control-Coherent Koopman Model (8) can be constructed for a dynamical system with an actuation subsystem that is linear in actuation.

**Theorem** [Control-Coherent Koopman Model]

If the dynamical system (1) has an actuation subsystem that is linear in actuation in the form of (14), and if observables  $\{g_i\}_{i=1}^{\infty}$  satisfying conditions (3) exist and they include the state variables of the actuation subsystem,  $p$ , in the observables, then the Control-Coherent Koopman Model of (1) is given by

$$z_{t+1} = Az_t + Bu_t. \quad (8)$$

where  $A$  is the Koopman operator of the associated autonomous system

$$\tilde{p}_{t+1} = h(x_t) \quad (16)$$

$$q_{t+1} = f_q(x_t) \quad (12)$$

which is valid in the compact set  $X$ , and the control matrix  $B$  is given by

$$B = \begin{bmatrix} B_p \\ 0 \end{bmatrix}. \quad (17)$$

**Proof:** Without loss of generality, we assume that the first  $m$  observables are the state variables of the actuation subsystem.

$$z_t = \begin{bmatrix} p_t \\ y_t \end{bmatrix} \quad (18)$$

where  $p_t = (g_1, \dots, g_m)^T$  and  $y_t = (g_{m+1}, g_{m+2}, \dots)^T$ .

Then the Koopman Operator for the autonomous system (12) and (16) exists and can be expressed as

$$\begin{bmatrix} \tilde{p}_{t+1} \\ y_{t+1} \end{bmatrix} = \begin{bmatrix} A_{pp} & A_{py} \\ A_{yp} & A_{yy} \end{bmatrix} \begin{bmatrix} p_t \\ y_t \end{bmatrix} \quad (19)$$

where the matrix and vectors are divided into blocks associated to the state of the actuator dynamics and the rest of the observables,  $y$ . Substituting  $\tilde{p}_{t+1} = p_{t+1} - B_p u_t$  into (19) and moving the term  $B_p u_t$  to the right-hand side yields

$$\begin{bmatrix} p_{t+1} \\ y_{t+1} \end{bmatrix} = \begin{bmatrix} A_{pp} & A_{py} \\ A_{yp} & A_{yy} \end{bmatrix} \begin{bmatrix} p_t \\ y_t \end{bmatrix} + \begin{bmatrix} B_p \\ 0 \end{bmatrix} u_t \quad (20)$$

This is the Control-Coherent Koopman Model of the non-autonomous, nonlinear dynamical system (1).

**Remark 3**

The Koopman operator given by (19) must be valid in the compact set  $X$ . Especially, the dynamic range of  $p$  must include all the states of  $p$  that can be driven by the input  $B_p u_t$ .

**Remark 4**

The above state equation (20) manifests that the actuator input  $u_t$  drives the actuator subsystem state to  $p_{t+1}$  and that all others in  $y$  are affected through  $p_{t+1}$  at the *next cycle*,  $t + 2$ . This causal sequence agrees with our observation and the causality analysis of physical modeling theory [17]. The causality dictates that the impact of the input  $u_t$  is captured and confined within the actuator dynamics in the first cycle,  $t \rightarrow t + 1$ , before being transmitted to the dynamics of  $y_t$  in the second cycle,  $t + 1 \rightarrow t + 2$ . If the actuator state  $p_t$  is eliminated, it implies that this transmission delay is eliminated. As a result, (11) becomes algebraic and the input is directly involved in (12), which prevents the application of Koopman Operator. The actuation subsystem must possess independent state variables.

If the linearity in actuation (14) is satisfied globally, in other words, the original dynamical system (1) is linear in control, the problem is straightforward. In most nonlinear dynamical systems, however, linearity in control occurs only for actuator subsystems. Considering the actuation subsystem is essential to fill the gap between the original Koopman operator theory for autonomous systems and real-world control systems.

#### IV. APPLICATION TO ROBOT ARM DYNAMICS

The Control-Coherent Koopman Modeling method is applicable to a broad spectrum of nonlinear dynamical systems. In this section and the following, two exemplary case studies will be described to demonstrate how the method is applied to practical problems.

Consider the equations of motion (EoM) of an  $N$  degree-of-freedom (DoF) robot in joint coordinates  $\theta \in \mathcal{R}^N$ .

$$H(\theta)\ddot{\theta} + C(\theta, \dot{\theta})\dot{\theta} + G(\theta) = \tau_j \quad (21)$$

where  $H(\theta)$  is an  $N \times N$  inertia matrix,  $C(\theta, \dot{\theta})\dot{\theta}$  is the Coriolis and centrifugal matrix,  $G(\theta)$  is the gravity vector, and  $\tau_j \in \mathcal{R}^N$  is the joint torque vector. If we define  $\theta$  and  $\dot{\theta}$  to be independent state variables, the state equation can be given by

$$\frac{d}{dt} \begin{pmatrix} \theta \\ \dot{\theta} \end{pmatrix} = \begin{bmatrix} \dot{\theta} \\ H(\theta)^{-1} \tau_j - H(\theta)^{-1} (C\dot{\theta} + G(\theta)) \end{bmatrix} \quad (22)$$

In most robotics literature, joint torques  $\tau_j(t)$  are treated as control input. In consequence, the state equation is not linear in control; the joint torques are multiplied by the inverse of the state-dependent inertia matrix,  $H(\theta)^{-1}$ . The Koopman operator

theory cannot be applied to this form of dynamical system.

Here, we apply the Control-Coherent Koopman Modeling based on actuator dynamics. Joint torques  $\tau_j(t)$  pertain to the dynamics of actuators driving individual joints. As shown in Fig. 1, let  $\phi_i$  be the rotor displacement of the actuator driving the  $i^{th}$  joint,  $\tau_{mi}$  the actuator torque,  $b_i$  the damping constant, and  $I_i$  the rotor inertia. Then, the following equation of motion is obtained,

$$\ddot{\phi}_i = \frac{1}{I_i}\tau_{mi} - \frac{1}{I_i}b_i\dot{\phi}_i - \frac{1}{I_i}\tau_{load,i}, \quad 1 \leq i \leq N \quad (23)$$

where  $\tau_{load,i}$  is the load torque from the  $i^{th}$  joint. Note that the local dynamics of this actuator are linear in control. This is true for most electro-mechanical robotic systems, because the inertia of each actuator's moving part, e.g. a motor rotor, has a constant inertia.

As shown in Fig.1, the power train of each joint actuator, comprising a gearing and transmission mechanism, inevitably possesses some torsional compliance. Suppose that a gear reducer of gear ratio  $1:r_i$  connects the actuator shaft and the joint axis with a torsional stiffness  $k_i$ , then the joint torque  $\tau_{ji}$  and the load torque  $\tau_{load,i}$  are related as

$$\tau_{ji} = r_i\tau_{load,i} = r_i k_i(\phi_i - r_i\theta_i). \quad (24)$$

where  $\theta = (\theta_1, \theta_2, \dots, \theta_N)^T$  and  $\phi = (\phi_1, \phi_2, \dots, \phi_N)^T$ .

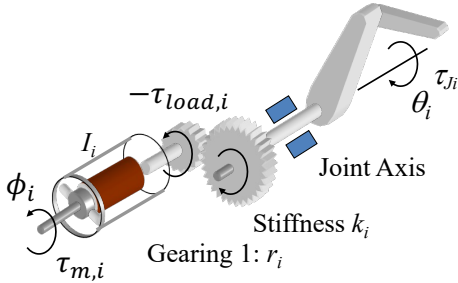


Fig. 1 Dynamic modeling of the  $i^{th}$  joint actuator with torsional compliance at the power train

With the compliance at the gearing,  $\phi_i$  and  $\theta_i$  become independent generalized coordinates. In discrete time, the independent state variables  $x_t = (p_t^T, q_t^T)^T$  are those of the actuators and the arm linkage, respectively.

$$p_t = \begin{bmatrix} \phi_t \\ \dot{\phi}_t \end{bmatrix}, \quad q_t = \begin{bmatrix} \theta_t \\ \dot{\theta}_t \end{bmatrix} \quad (25)$$

Using (24) in (22), the state equation of the arm linkage can be approximated to the following form in discrete time.

$$\begin{aligned} \theta_{t+1} &= \theta_t + \Delta t \dot{\theta}_t \\ \dot{\theta}_{t+1} &= \dot{\theta}_t + \Delta t H(\theta_t)^{-1} [\mathbf{r} \mathbf{k}(\phi_t - \mathbf{r} \theta_t) - C \dot{\theta}_t - G(\theta_t)] \end{aligned} \quad (26)$$

where  $\mathbf{r} = \text{diag}(r_1, \dots, r_N)$  and  $\mathbf{k} = \text{diag}(k_1, \dots, k_N)$ . Using (24) in (23) yields

$$\begin{aligned} \phi_{t+1} &= \phi_t + \Delta t \dot{\phi}_t \\ \dot{\phi}_{t+1} &= \dot{\phi}_t - \Delta t I^{-1} [\mathbf{b} \dot{\phi}_t + \mathbf{k}(\phi_t - \mathbf{r} \theta_t)] + \Delta t I^{-1} \tau_m \end{aligned} \quad (27)$$

where  $I = \text{diag}(I_1, \dots, I_N)$  and  $\mathbf{b} = \text{diag}(b_1, \dots, b_N)$ . The control input term  $\tau_m = (\tau_{m1}, \dots, \tau_{mN})^T$  are linearly involved in the actuator dynamics. Moving the linear control term to the left-hand side, the second equation becomes.

$$\dot{\phi}_{t+1} = \dot{\phi}_t - \Delta t I^{-1} [\mathbf{b} \dot{\phi}_t + \mathbf{k}(\phi_t - \mathbf{r} \theta_t)] \quad (28)$$

where  $\ddot{\phi}_{t+1} = \dot{\phi}_{t+1} - \Delta t I^{-1} \tau_m$ .

The Koopman operator  $A$  is computed for the autonomous system, (26) and (28). Using the resultant  $A$  matrix, the Control-Coherent Koopman Model (8) can be obtained by moving the control term  $\Delta t I^{-1} \tau_m$  to the right-hand side.

It should be noted that the actuator dynamics (27) is linear in this model. Therefore, unlike the arm linkage dynamics (26), which must be lifted with many observables for linearization, the actuator dynamics (27) does not need to lift, since it is already linear. This implies that the upper block matrices in (20),  $A_{pp}$ ,  $A_{py}$ , can be replaced by the parameters involved in (27) and that the coefficients associated to the observables for lifting linearization are all 0.

$$\begin{bmatrix} p_{t+1} \\ y_{t+1} \end{bmatrix} = \begin{bmatrix} \bar{A}_{pp} & \bar{A}_{px} & 0 & \dots & 0 \\ A_{yp} & A_{yy} & & & \end{bmatrix} \begin{bmatrix} p_t \\ y_t \end{bmatrix} + \begin{bmatrix} B_p \\ 0 \end{bmatrix} u_t \quad (29)$$

## V. APPLICATION TO MULTI-CABLE MANIPULATION

The Koopman operator theory can be applied to complex systems where governing equations of motion must be switched depending on the state location. Despite the switched nature of dynamics, the Koopman operator can provide a unified, globally linear model [12]. A multi-cable crane system is such an example, where the dynamics are switched depending on which cable is taut or goes slack. Multi-cable crane systems are capable of positioning, transportation, assembly, tumbling, and juggling of an object suspended with multiple cables.

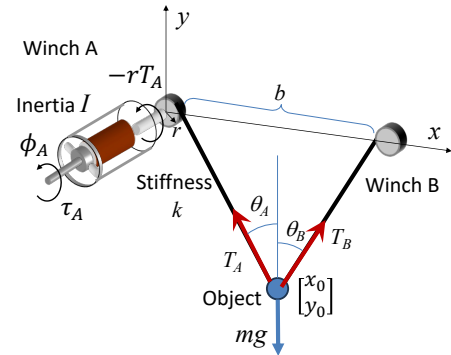


Fig.2 Two-cable manipulation with two winches

Fig.2 shows its simplest system consisting of two cables, two winches, and a point mass. Although the configuration is simple, the system exhibits complex nonlinear dynamics due to the uni-directional load-bearing property of cables. When a compressive load acts, the cable goes slack. Depending on the dynamic state, cables may be taut or slack, repeating taut-slack switching. Assuming some tensile compliance of each cable,



the taut-slack switching can be modeled as a continuous system. However, the governing equations have four facets depending on the taut-slack conditions of the two cables. The Koopman operator can provide a global, unified representation of this type of cable suspension system [12].

Let  $x_0$  and  $y_0$  be coordinates of the point mass  $m$ ,  $T_A$  and  $T_B$  be cable tensions of the two cables, respectively. When both cables are taut, the equations of motion are given by

$$\begin{aligned} m\ddot{x}_0 &= T_A \cos\theta_A - T_B \cos\theta_B \\ m\ddot{y}_0 &= T_A \sin\theta_A + T_B \sin\theta_B - mg \end{aligned} \quad (30)$$

where  $\theta_A$  and  $\theta_B$  are, respectively, angles of the two cables, which are functions of  $x_0$  and  $y_0$  (Fig.2). As a cable goes slack, the cable tension becomes zero and the term vanishes. When both cables are slack, the dynamic behavior becomes that of a projectile object. If we treat cable tensions,  $T_A$  and  $T_B$ , as control inputs, the system is nonlinear in control, and the Koopman operator cannot be applied.

Cable tensions pertain to the dynamics of the two winches. Assuming simple winch motors, the actuator dynamics are linear in actuator torques,  $\tau_A$  and  $\tau_B$ .

$$\begin{aligned} \ddot{\phi}_A &= \frac{1}{I} \tau_A - \frac{r}{I} T_A(x_0, y_0, \phi_A) \\ \ddot{\phi}_B &= \frac{1}{I} \tau_B - \frac{r}{I} T_B(x_0, y_0, \phi_B) \end{aligned} \quad (31)$$

where  $r$  is the radius of the winch pully,  $I$  the inertia of the winch rotor, and  $\phi_A$  and  $\phi_B$  are displacements of the two winch motors, respectively. Note that the cable tensions  $T_A$  and  $T_B$  are functions of the point mass location and the displacement of the winch motor. In the real multi-cable crane system, the cables have some compliance. Then, the point-mass coordinates,  $x_0$  and  $y_0$ , and the winch displacements,  $\phi_A$  and  $\phi_B$ , become independent generalized coordinates. Incorporating the state variables of the winch actuators and those of the point mass, we can construct a Koopman model that is linear in control, i.e. the new control,  $\tau_A$  and  $\tau_B$ , are linearly involved. Note that the local actuator dynamics are nonlinear in independent state variables but are linear in control. These meet the requirements for applying the Control-Cohesive Koopman modeling.

## VI. NUMERICAL SIMULATION

### A. The Two-Cable Crane

Fig.3 shows the simulation experiment of the two-cable crane system. First, the nonlinear dynamic model of the two-cable system was simulated and 500 trajectories starting from various initial conditions and control inputs were created. From these data, the Koopman model of the associated autonomous system predicting  $y_{t+1}$  and  $\dot{\phi}_{t+1} = \dot{\phi}_t - \Delta t I^{-1} \tau_m$  from  $y_t$  and  $p_t$  was obtained. The gray broken line in Fig.3 indicates the predicted trajectory starting at initial position (0.16 m, 0 m). The length of both cables was initially 0.53 m, while the distance between the two winches is 0.16 m. Therefore, both cables were initially slack. In the figure, the point mass initially

drops vertically and then bounces left when the left cable became taut. In this autonomous system, the trajectory was created with zero control inputs, i.e. the winch actuator torques were kept zero. The cables become longer as the point mass bounced several times.

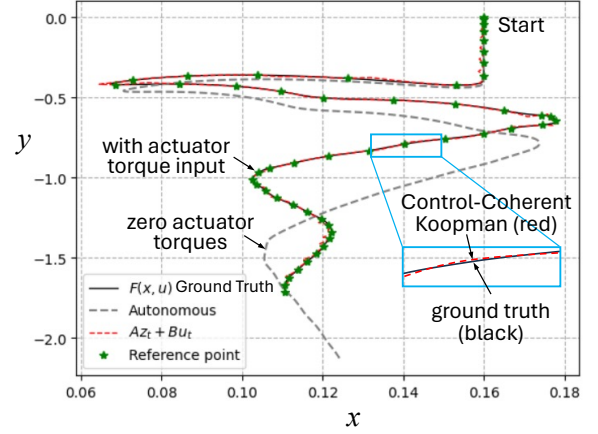


Fig.3 Comparison of Control-Coherent Koopman model to the ground-truth nonlinear system with control

The Control-Coherent Koopman model was obtained from this autonomous model by adding the linear control term. The red broken line in Fig.3 is the trajectory of the Koopman model when actuator torques are generated at the winch actuators. Note that this Control-Coherent Koopman model agrees almost perfectly with its ground truth: the solid black line obtained from the original nonlinear dynamics with the same control input. Also note that, in this example, the actuator dynamics are nonlinear in state but are linear in control. Although the actuator dynamics are nonlinear, the proposed method is applicable as long as the control terms are linearly involved.

### B. A Two-Link Robot Arm

Fig. 4 shows the tracking capabilities of a two-link robotic arm when applying Model Predictive Control (MPC) to follow a desired trajectory using the Control-Coherent Koopman model described previously.

The first link measures 1 m and weighs 5 kg, while the second link is 0.8 m and 4 kg. The arm moves in a horizontal plane with no gravity. The order of the arm dynamics is 4 for the 2 links, and that of the actuator dynamics is 4. In addition, 200 RBFs are used as observables, where the center locations are determined with the k-means clustering method.

The  $A$  matrix of the Control-Coherent Koopman model  $A_{CKK}$  is obtained with data containing both the autonomous ( $u_t = 0$ ) and non-autonomous ( $u_t \neq 0$ ) response of the system.

For comparison, a lifted Koopman model is constructed based on DMDc (9) ( $A_{DMDc}, B_{DMDc}$ ), using the same data and the same observables with the same centers and dilation factors as in the Control-Coherent Koopman model. The histogram of one-step ahead state prediction is shown in Fig. 5 for both Control-Coherent Koopman and DMDc.

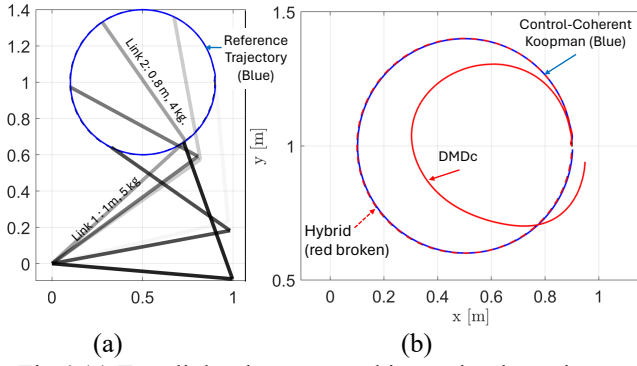


Fig.4 (a) Two-link robot arm tracking a circular trajectory based on Control-Coherent Koopman. (b) MPC control comparison of Control-Coherent Koopman (blue), DMDc (solid red), and a hybrid of  $A_{DMDc}$  and  $B_{CCK}$  (broken red).

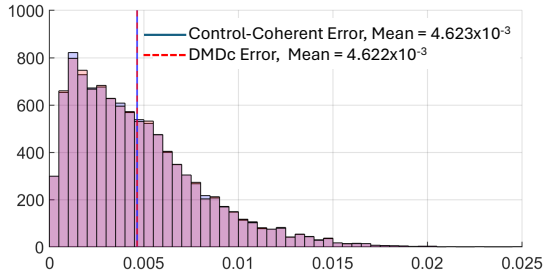


Fig.5 Histogram comparison shows almost identical prediction accuracy between Control-Coherent Koopman and DMDc

Note that the prediction error histogram is essentially the same for Control-Coherent Koopman and DMDc. Nonetheless, the MPC tracking performance is strikingly different. The Control-Coherent Koopman can accurately track the circular trajectory as shown in Fig.4-(a), while the DMDc failed to track it (b). This behavior is consistent; similar results were observed for diverse tracking trajectories and parameter values. Control-Coherent Koopman significantly outperformed DMDc for diverse RBF structure, dilation factor, and trajectory.

The main difference between the two approaches comes from how the B matrix is obtained. While the B matrix of Control-Coherent Koopman has non-zero elements only in the block of actuator dynamics (25), DMDc produces non-zero elements in both blocks. The  $B_{DMDc}$  allows the control input, i.e. actuator torques, to change the joint angles directly and instantaneously, which is not coherent with the physical model. They can only influence the transition of the velocities. When the MPC generates control signals based on the  $B_{DMDc}$  and applies them to the plant, it performs poorly.

Although the discrepancy between the two matrices seems insignificant, when applied to the MPC problem, it has a profound effect on the tracking performance. This is evident when, as an experiment, MPC is run with the A matrix from DMDc ( $A_{DMDc}$ ) but with the B matrix from Control-coherent Koopman ( $B_{CCK}$ ). The improvement on the tracking performance is significant as seen in Fig. 4-(b). This highlights the importance of Control-Coherent Koopman to lift nonlinear control systems, since it is only by the introduction of the actuator dynamics that the structure of the B matrix can be clearly defined.

## ACKNOWLEDGMENT

The authors thank Dr. Itta Nozawa of Sumitomo Heavy Industries for his assistance in numerical computation.

## REFERENCES

- [1] A. Mauroy and J. Goncalves, "Koopman-Based Lifting techniques for Nonlinear Systems Identification", IEEE Transactions on Automatic control, Vol.65, No.6, pp.2550-2565, 2019.
- [2] M. Korda and I. Mezic, "Linear Predictors for Nonlinear Dynamical Systems: Koopman operator Meets Model Predictive Control", Automatics, Vol. 93, pp.149-160, 2018.
- [3] M. Han, J. Euler-Rolle, and R.K. Katzschmann, "Descro: Stability-Assured Robust Control with a Deep Stochastic Koopman Operator", Proc. of International Conference on Learning Representations, 2021.
- [4] D. Bruder, X. Fu, R.B. Gillespie, C.D. Remy, and R. Vasudevan, "Data-Driven Control of Soft Robots Using Koopman Operator Theory", IEEE Trans. of Robotics, Vol.37, No.3, pp948-961, 2021.
- [5] V. Cibulka, T. Hanis, M. Korda, and M. Hromcik, "Model Predictive Control of a Vehicle Using Koopman Operator", IFAC Papers Online, Vol.53, No.2 pp.4228-4233, 2020.
- [6] I. Abraham and T. Murphey, "Active Learning of Dynamics for Data-Driven Control Using Koopman Operator", IEEE Trans. on robotics, Vol.35, No.5, pp.1071-1083, 2019.
- [7] B. O. Koopman, "Hamiltonian Systems and Transformation in Hilbert Space", *Proceedings of the National Academy of Sciences*, 17-5, 315-318, (1931).
- [8] C. W. Rowley, I. Mezic, S. Bagheri, P. Schlatter, D.S. Henningson, Spectral Analysis of Nonlinear Flows, *Journal of Fluid Mechanics*, 641, 1-13, (2009).
- [9] J. L. Proctor, S. L. Brunton, and J. N. Kutz, Dynamic Mode Decomposition with Control, *SIAM Journal of Applied Dynamical Systems*, 15-1, 142-161, (2016).
- [10] J. Proctor, S. Brunton, and N. Kutz, "Generalizing Koopman Theory to Allow for Inputs and Control", *SIAM Journal of Applied Dynamical Systems*, Vol.17, No.1, pp.909-930, (2018).
- [11] D. Bruder, X. Fun, and R. Vasudevan, "Advantages of Bilinear Koopman Realizations for the Modeling and Control of Systems With Unknown Dynamics", IEEE Robotics and Automation Letters, Vol.6, No.3 pp.4369 - 4376, July (2021).
- [12] H. Asada, "Global, Unified Representation of Heterogenous Robot Dynamics Using Composition Operators: A Koopman Direct Encoding Method", IEEE/ASME Transactions on Mechatronics, Vol.28, Issue 5, pp. 2633-2644, Digital Object Identifier: 10.1109/TMECH.2023.3253599, February (2023).
- [13] Q. Li, F. Dietrich, E. M. Bollt, and I. G. Kevrekidis, "Extended dynamic mode decomposition with dictionary learning: A data-driven adaptive spectral decomposition of the Koopman operator," *Chaos: An Interdisciplinary Journal of Nonlinear Science*, vol. 27, no. 10, (2017).
- [14] B. Lusch, J. N. Kutz, and S. L. Brunton, "Deep learning for universal linear embeddings of nonlinear dynamics," *Nature Communications*, vol. 9, no. 1, (2018).
- [15] E. Yeung, S. Kundu, and N. Hodas, "Learning deep neural network representations for koopman operators of nonlinear dynamical systems," in 2019 American Control Conference (ACC), pp. 4832-4839, (2019).
- [16] Y. Han, W. Hao, and U. Vaidya, "Deep learning of Koopman representation for control," in 2020 59th IEEE Conference on Decision and Control (CDC), pp. 1890-1895, (2020).
- [17] D. Karnopp, D. Margolis, and R. Rosenberg, "System Dynamics: Modeling and Simulation of Mechatronic Systems - 3rd Edition", Wiley, (2000).